Synchronizability determined by coupling strengths and topology on complex networks

Jesús Gómez-Gardeñes,[1,2] Yamir Moreno,[1] and Alex Arenas[3]
[1]*Institute for Biocomputation and Physics of Complex Systems (BIFI), University of Zaragoza, Zaragoza 50009, Spain*
[2]*Departamento de Física de la Materia Condensada, University of Zaragoza, Zaragoza E-50009, Spain*
[3]*Departament d'Enginyeria Informàtica i Matemàtiques, Universitat Rovira i Virgili, 43007 Tarragona, Spain*
(Received 6 February 2007; published 22 June 2007)

We investigate in depth the synchronization of coupled oscillators on top of complex networks with different degrees of heterogeneity within the context of the Kuramoto model. In a previous paper [Phys. Rev. Lett. **98**, 034101 (2007)], we unveiled how for fixed coupling strengths local patterns of synchronization emerge differently in homogeneous and heterogeneous complex networks. Here, we provide more evidence on this phenomenon, extending the previous work to networks that interpolate between homogeneous and heterogeneous topologies. We also introduce details of the path towards synchronization for the evolution of clustering in the synchronized patterns. Finally, we investigate the synchronization of networks with modular structure and conclude that, in these cases, local synchronization is first attained at the most internal level of organization of modules, progressively evolving to the outer levels as the coupling constant is increased. The present work introduces parameters that are proved to be useful for the characterization of synchronization phenomena in complex networks.

DOI: 10.1103/PhysRevE.75.066106 PACS number(s): 89.75.Fb, 05.45.Xt

I. INTRODUCTION

Studies of the emergence of collective and synchronized dynamics in large ensembles of coupled units have been carried out since the beginning of the 1990s in different contexts and in a variety of fields, ranging from biology, ecology, and semiconductor lasers to electronic circuits [1–3]. Collective synchronized dynamics has multiple applications in technology and is a common framework to investigate the crucial features in the emergence of critical phenomena in natural systems. For instance, it is a relevant issue to fully understand some diseases that appear as the result of a sudden and undesirable synchronization of a large number of neuronal units [4]. Recently, synchronization phenomena have also been proved to be helpful outside the traditional fields where it applies, for instance, in sociology where it can be used to study the mechanisms leading to the formation of social collective behaviors [5,6].

Among the many models that have been proposed to address synchronization phenomena, one of the most successful attempts to understand them is due to Kuramoto [7,8], who capitalized on previous works by Winfree [9] and proposed a model system of nearly identical weakly coupled limit-cycle oscillators. The Kuramoto-model (KM) mean-field case corresponding to a uniform, all-to-all, and sinusoidal coupling is described by the equations of motion

$$\dot{\theta}_i = \omega_i + \frac{K}{N}\sum_{j=1}^{N} \sin(\theta_j - \theta_i) \quad (i = 1, \ldots, N). \tag{1}$$

where the factor $1/N$ is incorporated in order to ensure a good behavior of the model in the thermodynamic limit, $N \to \infty$, ω_i stands for the natural frequencies of the oscillators, and K is the coupling constant. Moreover, the coherence of the population of N oscillators is measured by the complex order parameter,

$$r(t)\exp(\mathrm{i}\phi(t)) = \frac{1}{N}\sum_{j=1}^{N} \exp[\mathrm{i}\theta_j(t)], \tag{2}$$

where the modulus $0 \leqslant r(t) \leqslant 1$ measures the phase coherence of the population and $\phi(t)$ is the average phase. In what follows, we will focus on the synchronization of coupled oscillators described by the dynamics, Eq. (1), because of its validity as an approximation for a large number of nonlinear equations and its ubiquity in the nonlinear literature [10].

The KM approach to synchronization was a great breakthrough for the understanding of the emergence of synchronization in large populations of oscillators; in particular, it presents a second-order phase transition from incoherence to synchronization, in the order parameter, Eq. (2), for a critical value of the coupling constant. However, a large amount of real systems do not show a homogeneous pattern of interconnections among their parts [11,12] where the original KM assumptions apply.

Many real natural [13,14], social [15], and technological [16–18] systems conform as networks of nodes with connectivity patterns that diverge considerably from homogeneity and are usually characterized by a scale-free degree distribution $P(k) \sim k^{-\gamma}$ (the degree k is the number of connections of a node). The study of processes taking place on top of scale-free networks has led to a reconsideration of classical results obtained for regular lattices or random graphs due to the radical changes of the system's dynamics when the heterogeneity of the connectivity patterns cannot be neglected [19–24]. In this case one has to deal with two sources of complexity, the nonlinear character of the dynamics and the complex structures of the substrate, which are usually entangled. A contemporary effort to attack this entangled problem was due to Watts and Strogatz, that in 1998, trying to understand the synchronization of cricket chirps, which show a high degree of coordination over long distances as though the insects where "invisibly" connected, end up with a semi-

nal paper [25] about the small-world connectivity property. This work was the seed of the modern theory of complex networks [11,12]. Nevertheless, the understanding of the synchronization dynamics in complex networks still remains a challenge.

In recent years, scientists have addressed the problem of synchronization on complex networks capitalizing on the master stability function (MSF) formalism [26] which allows one to study the stability of the *fully synchronized state* [27–34]. The MSF is the result of a linear stability analysis for a completely synchronized system. While the MSF approach is useful for obtaining insight into what is going on in the system as far as the stability of the synchronized state is concerned, it is not useful for knowing how partial synchronization is attained. To this end, one must rely on numerical calculations and explore the *entire phase diagram*. Surprisingly, there are only a few works that have dealt with a study of the whole synchronization dynamics in specific scenarios [35–40] as compared with those where the MSF is used, given that the onset of synchronization is richer in its behavioral repertoire than the state of complete synchronization.

In a previous work [41], we have shown how, for fixed coupling strengths, local patterns of synchronization emerge differently in homogeneous and heterogeneous complex networks, driving the process towards a certain degree of global synchronization following different paths. In this paper, we extend the previous work to different topologies, even those with modular structure, and report more results supporting the previous claim. First, we extend the analysis carried out in [41] to networks in which the degree of heterogeneity can be tuned between the two limits of random scale-free networks and random graphs with a Poisson degree distribution. Second, in order to obtain further insight into the role of the structural properties on the route towards complete synchronization, we study the same dynamics on top of networks with a nonrandom structure at the mesoscopic level—i.e., networks with communities. The results support the usefulness of the tools developed and highlight the relevance of synchronization phenomena to study in detail the relationship between structure and function in complex networks.

II. KM MODEL ON COMPLEX NETWORKS

Let us now focus on the paradigmatic Kuramoto model. In order to manage with the KM on top of complex topologies we reformulate Eq. (1) to the form

$$\frac{d\theta_i}{dt} = \omega_i + \sum_j \Lambda_{ij} A_{ij} \sin(\theta_j - \theta_i) \quad (i = 1, \ldots, N), \qquad (3)$$

where Λ_{ij} is the coupling strength between pairs of connected oscillators and A_{ij} is the connectivity matrix ($A_{ij}=1$ if i is linked to j and 0 otherwise). The original Kuramoto model introduced above assumed mean-field interactions so that $A_{ij}=1$, $\forall i \neq j$ (all-to-all) and $\Lambda_{ij}=K/N$, $\forall i,j$.

The first problem when dealing with the KM in complex networks is the definition of the dynamics. In the seminal paper by Kuramoto [7], Eq. (1), the coupling term on the right-hand side of Eq. (3) is an intensive magnitude. The dependence on the number of oscillators, N, is avoided by choosing $\Lambda_{ij}=K/N$. This prescription turns out to be essential for the analysis of the system in the thermodynamic limit $N \to \infty$. However, choosing $\Lambda_{ij}=K/N$ the dynamics of the KM in a complex network becomes dependent on N. Therefore, in the thermodynamic limit, the coupling term tends to zero except for those nodes with a degree that scales with N [42].

A second prescription consists of taking $\Lambda_{ij}=K/k_i$ (where k_i is the degree of node i) so that Λ_{ij} is a weighted interaction factor that also makes intensive the right-hand side of Eq. (3). This form has been used to solve the so-called *paradox of heterogeneity*, which states that the heterogeneity in the degree distribution, which often reduces the average distance between nodes, may suppress synchronization in networks of oscillators coupled symmetrically with uniform coupling strength [34].

Finally, the prescription $\Lambda_{ij}=K$ [39,43,44], which may seem more appropriate, also presents some conceptual problems because the sum on the right-hand side of Eq. (3) could eventually diverge in the thermodynamic limit if synchronization is achieved. To our understanding, the most accurate interpretation of the KM dynamics in complex networks should preserve the essential fact of treating the heterogeneity of the network independently of the interaction dynamics and, at the same time, should remain calculable in the thermodynamic limit. Taking into account these factors, the interaction Λ_{ij} in complex networks should be inversely proportional to the largest degree of the system, $\Lambda_{ij}=K/k_{max}=\lambda$, keeping in this way the original formulation of the KM valid in the thermodynamic limit (in SF networks $k_{max} \sim N^{1/(\gamma-1)}$). In addition, the same order parameter, Eq. (2), can be used to describe the coherence of the synchronized state. Since k_{max} is constant for a given network, the physical meaning of this prescription is a rescaling of the time units involved in the dynamics. Note, however, that for a proper comparison of the synchronizability of different complex networks, the global and local measures of coherence should be represented according to their respective time scales. Therefore, given two complex networks A and B with $k_{max}=k_A$ and $k_{max}=k_B$, respectively, the comparison between observables must be done for the same effective coupling $K_A/k_A=K_B/k_B=\lambda$. With this formulation in mind Eq. (3) reduces to

$$\frac{d\theta_i}{dt} = \omega_i + \lambda \sum_j A_{ij} \sin(\theta_j - \theta_i) \quad (i = 1, \ldots, N), \qquad (4)$$

independently of the specific topology of the network. This allow us to study the dynamics of Eq. (4) over different topologies in order to compare the results and properly inspect the interplay between topology and dynamics in what concerns to synchronization.

III. HOMOGENEOUS vs HETEROGENEOUS TOPOLOGIES

Recent results have shed light on the influence of the local interactions' topology on the route to synchronization

[36,40]. However, in these studies at least two parameters (clustering and average path length) vary along the studied family of networks. This paired evolution, although yielding an interesting interplay between the two topological parameters, makes it difficult to distinguish what effects were due to one or other factors. Here, we would like to address first what is the influence of heterogeneity, keeping the number of degrees of freedom to a minimum for the comparison to be meaningful. The family of networks used in the present section are comparable in their clustering, average distance, and correlations so that the only difference relies on the degree distribution, ranging from a Poissonian type to a scale-free distribution. Later on in this paper, we will relax these constraints and study networks in which the main topological feature is given at the mesoscopic scale—i.e., networks with community structure.

Therefore, let us first scrutinize and compare the synchronization patterns in Erdös-Rényi (ER) and scale-free (SF) networks. For this purpose we make use of the model proposed in [45], which allows a smooth interpolation between these two extremal topologies. Besides, we introduce a parameter to characterize the synchronization paths to unravel their differences. The results reveal that the synchronizability of these networks does depend on the coupling between units and, hence, that general statements about their synchronizability are eventually misleading. Moreover, we show that even in the incoherent solution $r=0$, the system is self-organizing towards synchronization. We will analyze in detail how this self-organization is attained.

The first numerical study about the onset of synchronization of Kuramoto oscillators in SF networks [39] revealed the great propensity of SF networks to synchronization, which is revealed by a nonzero but very small critical value λ_c [46]. Besides, it was observed that at the synchronized state $r=1$, hubs are extremely robust to perturbations since the recovery time of a node as a function of its degree follows a power law with exponent -1. However, how do SF networks compare with homogeneous networks and what are the roots of the different behaviors observed?

We first concentrate on global synchronization for the Kuramoto model, Eq. (4). For this we follow the evolution of the order parameter r, Eq. (2), as λ increases, to capture the global coherence of the synchronization in networks. We will perform this analysis on the family of networks generated with the model introduced in [45]. This model generates a one-parameter family of networks labeled by $\alpha \in [0,1]$. The parameter α measures the degree of heterogeneity of the final networks so that $\alpha=0$ corresponds to the heterogeneous Barabási-Albert (BA) network and $\alpha=1$ to homogeneous ER graphs. For intermediate values of α one obtains networks that have been grown, combining both preferential attachment and homogeneous random linking so that each mechanism is chosen with probabilities $(1-\alpha)$ and α, respectively. It is worth stressing that the growth mechanism preserves the total number of links, N_l, and nodes, N, for a proper comparison between different values of α. Specifically, assuming the final size of the network to be N, the network is built up starting from a fully connected core of m_0 nodes and a set $\mathcal{S}(0)$ of $N-m_0$ unconnected nodes. Then, at each time step, a new node (not selected before) is chosen from $\mathcal{S}(0)$ and linked to m other nodes. Each of the m links is attached with probability α to a randomly chosen node (avoiding self-connections) from the whole set of $N-1$ remaining nodes and with probability $(1-\alpha)$ following a linear preferential attachment strategy [47]. After repeating this process $N-m_0$ times, networks interpolating between the limiting cases of ER ($\alpha=1$) and SF ($\alpha=0$) topologies are generated [45]. Furthermore, with this procedure, the degree of heterogeneity of the grown networks varies smoothly between the two limiting cases.

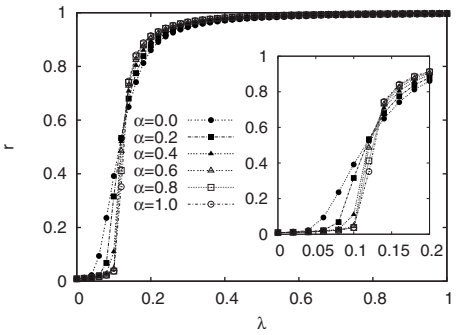

FIG. 1. Global synchronization curves $r(\lambda)$ for different network topologies labeled by α ($\alpha=0$ corresponds to the BA limit and $\alpha=1$ to ER graphs). The inset shows the region where the onset of synchronization takes place. The network sizes are $N=10^4$ and $\langle k\rangle=6$ ($N_l=3\times10^4$) and were generated using the model introduced in [45].

The curves $r(\lambda)$ for several network topologies ranging from ER to SF are shown in Fig. 1. We have performed extensive numerical simulations of Eq. (4) for each network substrate starting from $\lambda=0$ and increasing it up to $\lambda=0.4$ with $\delta\lambda=0.02$. A large number (at least 500) of different network realizations and initial conditions were considered for every value of λ in order to obtain an accurate phase diagram. The natural frequencies ω_i and the initial values of θ_i were randomly drawn from a uniform distribution in the interval $(-1/2,1/2)$ and $(-\pi,\pi)$, respectively.

Figure 1 reveals the differences in the critical behavior as a function of the substrate heterogeneity. The global coherence of the synchronized state, represented by r, shows that the onset of synchronization first occurs for SF networks. As the network substrate becomes more homogeneous the critical point λ_c shifts to larger values and the system seems to be less synchronizable. On the other hand, it is also clear that the route to complete synchronization, $r=1$, is faster for homogeneous networks. That is, when $\lambda>\lambda_c(\alpha)$ the growth rate of r increases with α. To inspect in depth the critical parameters of the system dynamics we perform a finite-size scaling (FSS) analysis. This allows us to determine with precision the curve $\lambda_c(\alpha)$ and study the critical behavior near the synchronization transition. We assume a scaling relation of the form

$$r = N^{-\nu} f(N^{\beta}(\lambda-\lambda_c)), \tag{5}$$

where $f(x)$ is as usual a universal scaling function bounded as $x\to\pm\infty$ and ν and β are critical exponents to be determined. The detailed analysis performed for both SF and ER

TABLE I. Topological properties of the networks used in this work and critical points for the onset of synchronization obtained from a FSS analysis [Eq. (5)]. The topological quantities reported are the result of an average over 1000 network realizations. $\langle k\rangle=4$ and $N=10^4$ have been set for all networks. Standard deviation of the mean values for λ_c is ±2 units in the last significant digit.

α	$\langle k^2\rangle$	k_{max}	λ_c
0.0 (SF)	115.5	326.3	0.051
0.2	56.7	111.6	0.066
0.4	44.9	47.7	0.088
0.6	41.1	25.6	0.103
0.8	39.6	16.8	0.108
1.0 (ER)	39.0	14.8	0.122

topologies shows that the critical value of the effective coupling, λ_c, corresponds in scale-free networks to $\lambda_c^{SF}=0.051$ and in random networks to $\lambda_c^{ER}=0.122$, accordingly with Fig. 1. In both cases, the transition strongly recalls the classical transition of the original KM [7] with a critical exponent near 1/2 for the SF network. In [39,40] two different techniques for a finite-size scaling analysis have been discussed, corroborating the findings here reported. For intermediate values of α, the results show that the critical point shifts to larger values as the degree of heterogeneity increases. They are shown in Table I together with some topological properties of the networks.

The differences between ER and SF topologies observed when looking at global patterns of synchronization motivate a more detailed study of the synchronization onset for both topologies. The original work by Kuramoto pointed out that at the onset of synchronization small clusters of locked oscillators emerge and that the recruitment of more oscillators into these clusters as the coupling is increased makes it larger the global coherence r of the system. Obviously the emergence of these clusters would depend on the underlying topology which drives the possible configurations that locked oscillators would eventually form. To see how this initial coherence is achieved we propose an order parameter r_{link}. This parameter measures the local construction of the synchronization patterns [48] and allows for the exploration of how global synchronization is attained. We define

$$r_{link}=\frac{1}{2N_l}\sum_i\sum_{j\in\Gamma_i}\left|\lim_{\Delta t\to\infty}\frac{1}{\Delta t}\int_{t_r}^{t_r+\Delta t}e^{i[\theta_i(t)-\theta_j(t)]}dt\right|, \quad (6)$$

Γ_i being the set of neighbors of node i. The parameter r_{link} measures the fraction of all possible links that are synchronized in the network. The averaging time Δt should be taken large enough in order to obtain good measures of the degree of coherence between each pair of physically connected nodes. Besides, r_{link} is computed after the system relaxes at some large time t_r. Note that in the limit of all-to-all coupling the information provided by r_{link} is exactly the same as the one provided by r because in this case $r_{link}\propto r^2$. Therefore, no additional information would be provided by this parameter in the all-to-all case. Here, however, it turns out to be the key

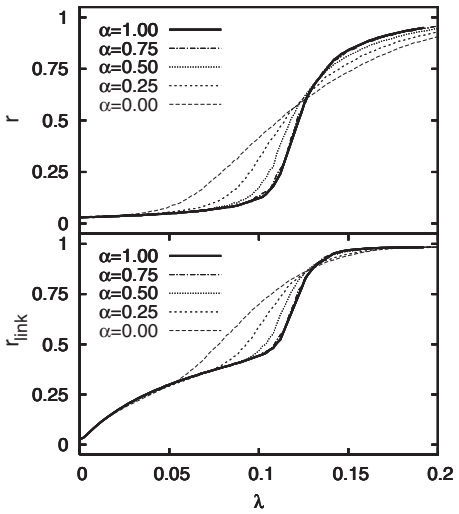

FIG. 2. Evolution of the control parameters r and r_{link} as a function of the coupling strength for networks generated with the model introduced in [45], corresponding to $\alpha=0.0$ (SF), 0.25, 0.5, 0.75, and 1.0 (ER). The size of the networks is $N=10^3$ and their average degree is $\langle k\rangle=6$. The exponent of the SF networks increases from $\gamma=3$ ($\alpha=0$).

parameter to characterize how synchronization emerges at a local scale.

In Fig. 2 we represent the evolution of both order parameters r and r_{link} as a function of the coupling strength λ for several values of α. The behavior of r_{link} shows a change in synchronizability between ER and SF and provides additional information to that reported by r. Interestingly, the nonzero values of r_{link} for $\lambda\leqslant\lambda_c$ indicate the existence of some local synchronization patterns even in the regime of global incoherence ($r\approx 0$). Right at the onset of synchronization for the SF network limit, its r_{link} value deviates from that of the ER, recovering the known result about the synchronization of SF networks for lower values of the coupling. In this region, while the synchronization patterns continue to grow for the ER network at the same rate, the formation of locally synchronized structures occurs at a faster rate in the SF network. Finally, when the incoherent solution in the ER network destabilizes, the growth of its synchronization pattern increases drastically up to values of r_{link} comparable to those obtained in SF networks and even higher. For intermediate values of α, the results show that the effect of varying the heterogeneity of the underlying network is twofold. On the one hand, the more heterogeneous the network is, the smaller the values of λ needed for the onset of synchronization. Conversely, the increase in the degree of heterogeneity results in larger values of λ in order to achieve complete synchronization. In short, as the heterogeneity is increased, the onset of synchronization is anticipated, but at the same time, the appearance of the fully synchronized state is delayed.

These results undoubtedly point out that statements about synchronizability are dependent on the coupling strength value. To shed light on this phenomenon, we have studied the characteristics of the synchronization patterns along the evolution of r_{link}. Following the usual picture, synchroniza-

tion patterns are formed by pairs of oscillators, physically connected, whose phase difference in the stationary state tends to zero. In order to determine which pairs of nodes are truly synchronized we should determine the coherence of their dynamics. Note that Eq. (6) is the average dynamical coherence between every pair of linked nodes and then the synchronization degree of every pair of connected oscillators can be written in terms of a symmetric matrix

$$\mathcal{D}_{ij} = A_{ij} \left| \lim_{\Delta t \to \infty} \frac{1}{\Delta t} \int_{t_r}^{t_r + \Delta t} e^{i[\theta_i(t) - \theta_j(t)]} dt \right| . \quad (7)$$

Then one has to analyze each matrix term D_{ij} in order to label a link (i,j) as synchronized or not. As introduced above, from the computation of r_{link} one determines the fraction of physical links that are synchronized so that one would expect that $2r_{link}N_l$ elements of the matrix $\mathcal{D}$ are $D_{ij}=1$, while the remaining elements are $D_{ij}=0$. However, this is not the real situation since the network dynamics is not well defined in terms of a fully synchronized cluster and a set of completely incoherent oscillators. On the other hand, the worst scenario would be found if there were $2N_l$ elements of matrix $\mathcal{D}$ so that $D_{ij}=r_{link}$, implying that all physically connected pairs are equally synchronized and hence the parameter r_{link} could not be interpreted as the fraction of links that are dynamically coherent and no information about the topological patterns of synchronization could be extracted from matrix $\mathcal{D}$. The situation found is not as simple as the former possibility and not so dramatic as the latter. The contributions D_{ij} of the N_l elements of matrix $\mathcal{D}$ that correspond to physical links can be ordered from the highest to the lowest one. We have checked that for two situations, corresponding to the onset of synchronization ($\lambda=0.05$), and when high global coherence ($\lambda=0.13$) is observed for a SF network, synchronized links can be clearly identified. For the onset of synchronization, a subset of nearly 20% of links displaying coherent dynamics with high degree of synchronization, $\mathcal{D}_{ij}>0.8$, is well separated from the behavior of the remaining links as a dramatic decrease of D_{ij} takes place. In this sense, it is clear that the dynamics of a 20% of the possible pairs can be regarded as synchronized which is in agreement with the obtained value $r_{link}=0.25$ for $\lambda=0.05$ and supports the observation that although macroscopic coherence is not observed ($r\simeq 0$ at this point), the system is seen to walk towards it. For $\lambda=0.13$ ($r_{link}\simeq 0.82$) a plateau of nearly 75% of links is observed, thus revealing the high degree of global coherence, $r\simeq 0.7$, at this point. Therefore, the shape of the ranked $\mathcal{D}_{ij}$ curves confirms that r_{link} gives the fraction of synchronized links and thus the latter allows one to obtain information about synchronized patterns from $\mathcal{D}$.

To determine exactly which pairs of nodes are regarded as synchronized, the matrix $\mathcal{D}$ is filtered using a threshold T such that the fraction of synchronized pairs equals r_{link}. In this way T is a moving threshold so that if $\mathcal{D}_{ij}>T$ oscillators i and j are considered synchronized. The value of T depends on the particular realization and is determined by means of an iterative scheme starting from $T=1$. Decreasing it with $\delta T=0.01$ one computes the amount of links that fulfill the condition. In this way, the value of T progressively decreases

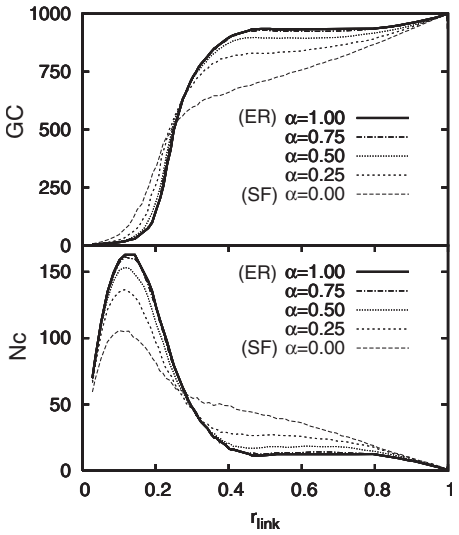

FIG. 3. Evolution of the number of synchronized clusters, N_c, and the synchronized giant component (GC) size as a function of r_{link} for the the different topologies considered. Small values of r_{link} correspond to values of λ for which $r\approx 0$. Despite r being vanishing and hence no global synchronization is yet attained, a significant number of clusters show up. This indicates that for any $\lambda>0$ the system self-organizes towards macroscopic synchronization. The network parameters are as in Fig. 2.

and more pairs of oscillators are chosen. The process lasts until T is such that the fraction of chosen links is equal to the desired value r_{link} previously computed from $\mathcal{D}$. Finally, when the synchronized links are identified the clusters of synchronized nodes are reconstructed.

Figure 3 represents the number of synchronized clusters and the size of the giant component (GC) as a function of r_{link} for the same values of α used in Fig. 2. The local information extracted from it points to a novel feature of the synchronization process that is not possible to derive from Figs. 1 and 2 and that is unexpected. The emergence of clusters of synchronized pairs of oscillators (links) in the networks shows that for values of λ for which the incoherent solution $r=0$ is stable, the networks have developed the largest cluster of synchronized pairs of oscillators involving 50% of the nodes and an equal number of smaller synchronization clusters. From this point on, the behavior of both GC and N_c depends on the specific value of α. When heterogeneity dominates, the GC grows and the number of smaller clusters goes down, whereas for less heterogeneous networks the growth of the GC is more abrupt and nodes are incorporated to it more faster. Moreover, the results highlight the fact that although heterogeneous networks exhibit more coherence in terms of r and r_{link}, the microscopic evolution of the synchronization patterns is faster in homogeneous networks, these networks being far more locally synchronizable than the heterogeneous ones once $\lambda>\lambda_c$.

The observed differences in the behavior at a local scale are rooted in the growth of the GC. For homogeneous topologies, many small clusters of synchronized pairs of oscillators (note in Fig. 3 the large number of clusters formed when 15% of the links are synchronized) merge together to form a GC when the effective coupling is increased. This

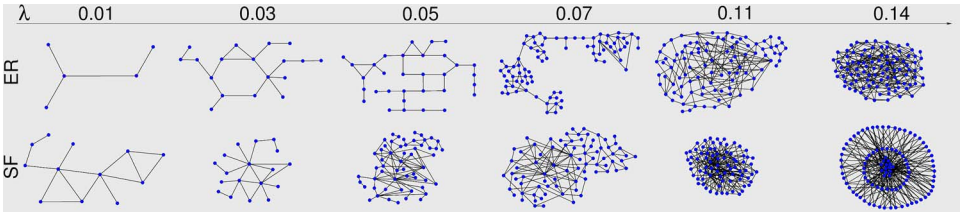

FIG. 4. (Color online) Giant synchronized components for several values of λ in the two limiting cases of the different topologies studied (ER and SF). The size of the underlying networks is small ($N=100$ nodes), in order to have a sizable picture of the system. Note that for the SF case links and nodes are incorporated together to the GC, while for the ER network, what is added are links between nodes already belonging to the GC.

coalescence of many small clusters results in a giant component made up of almost the size of the system once the incoherent state destabilizes. On the other hand, for heterogeneous graphs, the growth of the giant component is more smooth and the oscillators form new pairs starting from a core made up of half the nodes of the network. That is, in one case (ER-like networks), almost all the nodes of the network take part in the giant component from the beginning and later on, when λ is increased, what is added to the GC are the links among these nodes that were missing in the original cluster of synchronized nodes. For SF-like networks, the mechanism is the opposite. Nodes are added to the GC *together* with most of their links, resulting in a growth of r_{link} much slower than for the homogeneous topologies.

The above picture is confirmed in Fig. 4, where we have represented the evolution of the local synchronization patterns of the giant components in ER and SF networks for several values of λ [49]. It is clear that when $r \simeq 0$ the two networks follow different paths toward synchronization. In particular, the giant component for the SF network seems to retain the topological features of the substrate network, while this is not the case for the ER network (for instance, the small-world property is clearly lacking).

This study of the patterns of self-organization towards synchronization reveals that the quantitative difference between the macroscopic behaviors, shown by the computation of the evolution of the global coherence r for ER and SF networks, has its roots in a qualitatively different route at the microscopic level of description. The use of the parameter r_{link} which involves the computation of the degree of coherence between each pair of linked nodes is a useful tool for describing such differences. Moreover, the results suggest that the degree of heterogeneity of the network is the key ingredient to explain the two different routes observed. The technique developed to extract the synchronization patterns allows the analysis of the topological features of such clusters of nodes. We can compute the average measures of relevant quantities such as the clustering coefficient (which measures the density of small loops of length 3 in a network) and the degree distribution, and see how these magnitudes evolve from the uncoupled limit, where no synchronization occurs, to the coherent regime where the synchronized network coincides with the underlying substrate. It is then relevant to explore the regions where the onset of synchronization takes place and characterize topologically these emergent synchronized clusters.

In Fig. 5 the evolution of the average clustering coefficient $\langle c_{sync} \rangle$ of the giant synchronized cluster, referred to $\langle c_{network} \rangle$ in the underlying network, is plotted as a function of λ for both the BA and ER networks. It is worth mentioning that the results depicted in the figure have been computed taking into account that nodes with degree 1 do not contribute to the clustering coefficient of the GC, as c is not properly defined for these nodes. The results are illustrative of the local organization of synchronized nodes. The figure shows that for both topologies the clustering decreases as the coupling is increased beyond their respective λ_c or, in other words, as the giant component grows by the addition of new synchronized pairs of nodes. However, the effects of the two different routes to complete synchronization observed for ER and SF networks are well appreciated from the results. For the heterogeneous network there is a smooth decrease of the clustering coefficient for $\lambda > \lambda_c^{SF}$ and the effects of the emergence of global coherence are not dramatic in what refers to the behavior of $\langle c_{sync} \rangle$. This is because in this case the giant component mainly grows by recruiting new synchronized nodes and their links. On the other hand, for the ER graph the behavior observed for $\lambda < \lambda_c^{ER}$—i.e., when no macroscopic coherence is observed—is interrupted by a sudden jump near its critical value. In fact, for $\lambda > \lambda_c^{ER}$ the clustering of the synchronized cluster quickly approaches the value of $\langle c \rangle$ of the substrate network. This effect becomes clear if one has in mind the coalescence of small clusters, which happens around the critical point for ER graphs. In fact, taking into account the giant synchronized component on ER for $\lambda < \lambda_c^{ER}$ implies that one considers one of the several disjoint

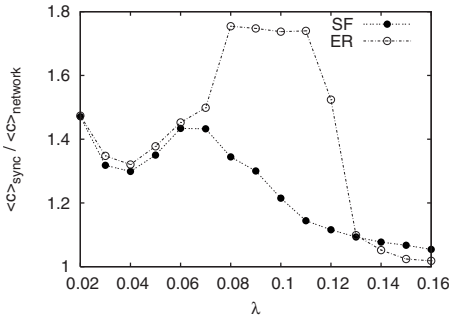

FIG. 5. Evolution of the ratio between the clustering coefficient of the giant synchronized cluster, $\langle c_{sync} \rangle$, and that of the substrate network, $\langle c_{network} \rangle$, as a function of λ for the two limiting cases of BA and ER networks. Network parameters are those used in Fig. 2.

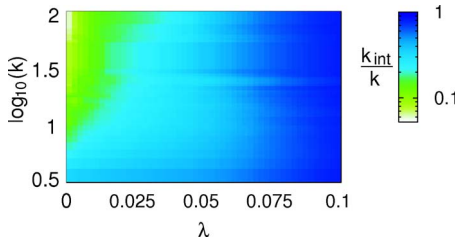

FIG. 6. (Color online) The plot shows the fraction of links that a node with degree k belonging to the synchronized cluster shares with other nodes of the same synchronized cluster. This fraction k_{int}/k is plotted as a function of $\log_{10}(k)$ and λ. The figure shows how the hubs progressively incorporate their neighbors to the synchronized component as λ grows. The network is SF with parameters as those used in Fig. 2 and $\alpha=0$.

synchronized clusters of similar sizes that are in this region. Moreover, the coalescence process leads to the formation of a giant cluster that contains almost all nodes of the network (see Fig. 3), but a number of links significantly smaller. Hence, when the clusters collapse into a much larger one, the topological features change dramatically as observed from the evolution of the clustering coefficient.

All the results reported above point out that the ultimate reason behind the two different routes to complete synchronization is the heterogeneous character of the SF network and the role played by the hubs. The natural cohesion that hubs provide to SF networks prevents the existence of independent macroscopic clusters of synchrony as occurs for ER networks. It is then interesting to study how these hubs participate in the formation of the final synchronized state. For this, we first study the evolution with λ of the composition of the synchronized cluster in terms of the degree of its components. In [41], we reported the probability that a node with degree k belongs to the giant synchronized cluster as a function of its degree k and the coupling λ for the SF network. This probability turns out to be an increasing function of k for every value of λ, and therefore the more connected a node is, the more likely it takes part in the cluster of synchronized links. In particular, the results confirm the hypothesis made above that the hubs participate from the very beginning on the formation of the synchronized cluster. A similar result was obtained in [51], where Zhou and Kurths studied the hierarchical organization in complex networks, using the MSF and a mean-field approach in the weak-coupling limit.

The above characterization of the synchronized cluster in terms of the degree of its component can be completed studying their effective degree k_{int}. The effective degree of a synchronized node is the number of links it shares with other nodes belonging to the same synchronized cluster. Obviously, at the complete synchronized regime a node with degree k will have $k_{int}=k$. We plot in Fig. 6 the quantity k_{int}/k (the fraction of links that a node has with synchronized neighbors) as a function of λ and the degree k of the nodes ($\alpha=0$). The results reveal that although hubs are the first to take part of the synchronized cluster, their neighbors are progressively incorporated into the cluster as λ grows. Besides, if a node with small k is synchronized, the probability that its neighbors are also synchronized grows very fast with λ, which is an effect of the network topology. These results further support the statement about the essential role played by the hubs in the recruitment of oscillators into the synchronized group and in the emergence of complete synchronization in SF networks.

IV. SYNCHRONIZATION IN STRUCTURED NETWORKS

In light of the results of the above section we have extended the study beyond unstructured networks to structured or modular networks. This is a limiting situation in which the local structure may greatly affect the dynamics, irrespective of whether or not we deal with homogeneous or heterogeneous networks, and then they constitute a perfect framework for testing the order parameter r_{link} introduced in the last section.

Many complex networks in nature are modular—i.e., composed of certain subgraphs with differentiated internal and external connectivity that form communities [12,50]. The use of modular networks where a proper comparison in synchronizability can be performed (same number of nodes and links) restricts us to the consideration of synthetic structured networks. To this end, we make use of a common benchmark of random network with community structure, first proposed by Newman [52] considering one hierarchical level and later extended to several hierarchical levels [37,38].

The modular network structure we build is as follows: in a set of N nodes, we prescribe n compartments that will represent our first community organizational level and m compartments, each one embedding four different compartments of the first level, which define the second organizational level of the network. The internal degree of nodes at the first level z_{in_1} and the internal degree of nodes at the second level z_{in_2} keep an average degree $z_{in_1}+z_{in_2}+z_{out}=\langle k\rangle$ so that these networks are strictly homogeneous in the sense of the degree distribution, $P(k)=\delta(k-\langle k\rangle)$. Networks with two hierarchical levels are labeled as $z_{in_1}-z_{in_2}$; e.g. a network with $i-j$ means i links with the nodes of its first hierarchical community level (more internal), j links with the rest of communities that form the second hierarchical level (more external), and $(\langle k\rangle-i-j)$ links with any community of the rest of the network.

Synchronization processes on top of modular networks of this type have been recently studied as a mechanism for community detection [37,53]. In [37], the authors studied the situation in which starting from a set of homogeneous (in terms of the natural frequencies) Kuramoto oscillators with different initial conditions the system evolves after a transient of time to the synchronized state. It was shown that the community structure is progressively unveiled at the same time the system's dynamics evolves toward the coherent state and the synchronization is attained. In particular, the nodes belonging to the first community level are the first to get synchronized, subsequently the second level nodes achieve the frequency entrainment, and finally the whole system shows global synchronization.

Here we adopt a different perspective since we will consider as previously a set of nonidentical Kuramoto oscillators

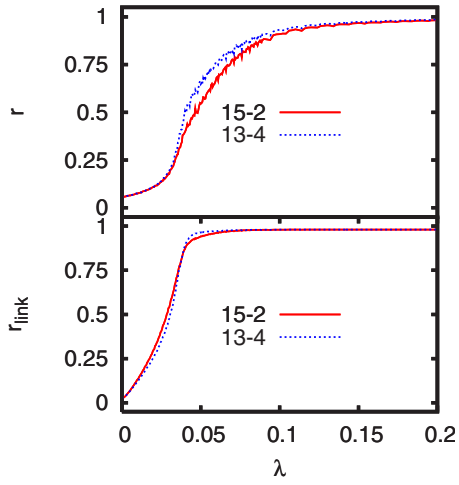

FIG. 7. (Color online) Evolution of r (top) and r_{link} (bottom) as a function of λ for structured modular networks. The networks are synthetically built with an *a priori* community structure. The network size is 256 nodes and the number of links is 4608. We prescribe 16 compartments that will represent our first community organizational level and four compartments, each one embedding four different compartments of the above first level, that define the second organizational level of the network. Each node has 18 links distributed between its first community level, the second, and the whole network at random. The network 13-4 has 13 internal connections in its first hierarchical level, 4 external connections in its second hierarchical level, and 1 connection with any other community in the network. The generation of the 15-2 structure is equivalent. The curves show that although 13-4 has always a better global synchronization, 15-2 has better local synchronization as shown by r_{link}.

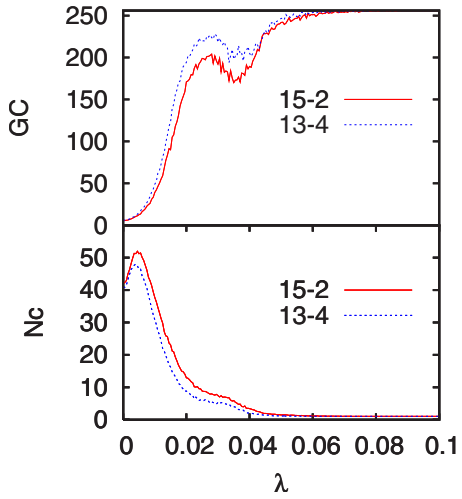

FIG. 8. (Color online) Size of the largest synchronized cluster GC and number of clusters, N_c, for the same networks of Fig. 7. See the text for details.

with random assignment of natural frequencies and hence the final degree of system's synchronization will depend on the strength of the coupling. It is then interesting to study how the degree of synchronization evolves as a function of λ and whether the coherence between nodes is progressively distributed following the hierarchy imposed by the underlying topology. For this, we make use of the order parameters r, Eq. (2), and r_{link}, Eq. (6), to characterize the synchronization transition of two slightly different modular networks with two well-defined hierarchical levels 13-4 and 15-2, this difference being the cohesion of the internal community core, 13 links out of 15 possible neighbors or 15 links (i.e., all-to-all) at the most internal level. Both networks have $N=256$ and $\langle k\rangle=18$. Figure 7 shows the results for both kinds of networks, revealing that the path towards synchronization as a function of the interaction is again affected by the structure. They also show that the information provided by r_{link} is essential to unveil the synchronization process. While the global synchronization parameter r is reflecting that the 13-4 structure globally synchronizes always better, r_{link} tells us again about the local synchronization. It shows that local synchronization is indeed favored in the 15-2 structure since r_{link} is larger for this topology for small values of λ where the system is locally forming synchronized clusters. This result, not captured by the macroscopic indicator r, is expected since the internal cohesion of communities at the first hierarchical level is larger for the 15-2 than for the 13-4. The evolution of r_{link} shows that when the coupling λ is increased the number of links synchronized in the 13-4 network becomes larger than in the 15-2 structure, revealing that complete synchronization is then favored by the presence of more external links connecting the first level communities.

Figure 8 shows the size of the giant component of synchronized clusters and the number of them as a function of λ. An interesting effect of the community structure of the networks and of the dynamics of the synchronization process is revealed in the figure. Right at the value of λ where the onset of global coherence takes place, the size of the GC suddenly falls, to increase again at larger values of the coupling strength. Additionally, note that this point coincides with that corresponding to a change in the concavity of the $r_{link}(\lambda)$ curves. This change at the microscopic level is due to the readjustment of links that connect synchronized nodes. In fact, as Fig. 9 illustrates for both networks, in this region of λ values, the number of links connecting synchronized nodes of the third level decreases while the number of those ascribed to the second level raises. That is, the synchronization process takes place in such a way that the first to synchronize are the nodes of the inner community level, then the second, and so on until the whole network gets synchronized. The relevant fact is that in order for r_{link} and r to grow, the nodes and links of the second level adjust their phases at the expense of those of the outer layer, the third level. This is also reflected in the number of clusters of synchronized links (N_c); i.e., the network appears as if the nodes of the third level were "temporarily" disconnected. Moreover, as the 13-4 network has more links connecting the first and second hierarchical levels, N_{links2} rises faster in this network than in the 15-2.

We have further inspected the synchronization path in modular networks. This can be easily done and visualized by the representation of the filtered matrix $\mathcal{D}$. It implies that one reassign the values of the matrix $\mathcal{D}$ so that $\mathcal{D}_{ij}=1$ if $\mathcal{D}_{ij}>T$ and $\mathcal{D}_{ij}=0$ otherwise. Plotting this filtered matrix for different values of the coupling λ one can easily determine which links are the first to synchronize since the form of the adja-

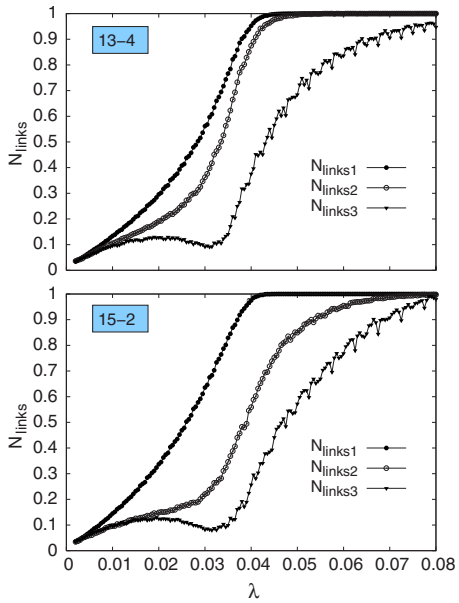

FIG. 9. (Color online) Number of links (N_{links}) that connect synchronized nodes in each of the three levels in the community hierarchy of the networks (1 means inner layer). The numbers are normalized by the total number of links at each level in each network.

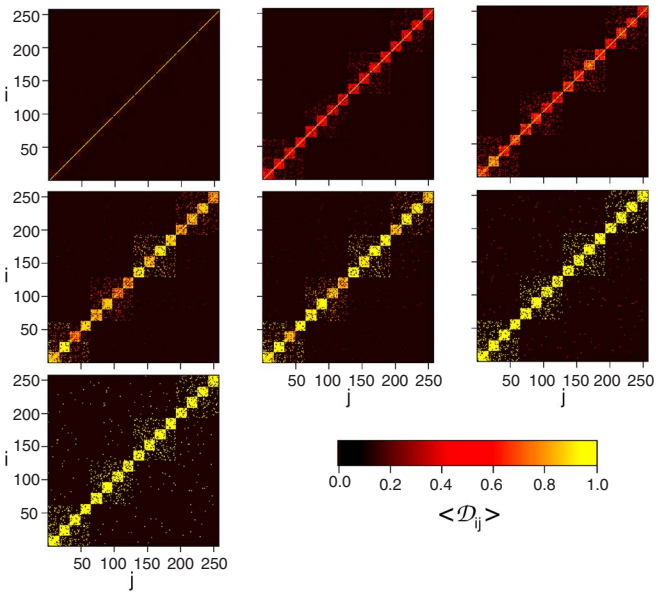

FIG. 10. (Color online) We represent the degree of synchronization between pairs of connected nodes for several values of the coupling λ in a 13-4 modular network (with two organizational levels) of $N=256$ nodes. The color code denotes the value of the averaged (over different initial conditions) filtered matrix $\langle \mathcal{D}_{ij} \rangle \in [0,1]$. The values of the coupling are (from left to right and top to bottom) $\lambda=0.011, 0.026, 0.032, 0.035, 0.038, 0.046, 0.210$ (corresponding to full synchronization). The pictures show that the order of synchronization is given by the organizational levels. The first community level is the first one to get synchronized; subsequently, second-level nodes attain synchronization for a larger value of λ; and finally, the full synchronized state is reached when outer links have $\langle D_{ij} \rangle = 1$.

cency matrix (which includes all physical links between nodes) is also easy to interpret because of its nested structure. Figure 10 shows how the community structure determines the internal organization of the system in the route towards full synchronization for the 13-4 network. For this study we have computed the value of the filtered matrix $\mathcal{D}$ for a number of initial conditions and then took its average value so that $\langle \mathcal{D}_{ij} \rangle \in [0,1]$ accounts for the synchronization strength of the network link (i,j). The results point out that link synchronization depends on the organizational level they belong to. Those connecting nodes belonging to the same first level community are the fastest (in terms of the coupling strength λ) to reach full synchronization. For larger values of λ full synchronization is attained progressively for the subsequent organizational levels. Then, one can conclude that the inner the link is the faster it gets synchronized in agreement with previous studies reported above [37].

V. CONCLUSIONS

In this paper we have explored several issues about synchronization in complex networks of Kuramoto phase oscillators. Our main concern has been the study of the synchronization patterns that emerge as the coupling between nonidentical oscillators increases. We have described the degree of synchronization between each pair of connected oscillators. The use of a parameter r_{link} allows us to reconstruct the synchronization clusters from the dynamical data. We have studied how the underlying topology (ranging from homogeneous to heterogeneous structures) affects the evolution of synchronization patterns. The results reveal that the route towards full synchronization depends strongly on whether one deals with homogeneous or heterogenous topologies. In particular, it has been shown that a giant cluster of synchronization in heterogeneous networks comes from a unique core formed by highly connected nodes (hubs) whereas for homogeneous networks several synchronization clusters of similar size can coexist. In the latter case, a coalescence of these clusters is observed in the synchronization path which is macroscopically manifested by the sudden growth of global coherence. Another important effect of the underlying topology is manifested in an anticipated onset of global coherence for heterogeneous networks with respect to more homogeneous topologies. However, the latter reaches the state of full synchronization at lower values of the coupling strength, therefore showing that statements about the synchronizability of complex networks are relative to the region of the phase diagram where they operate. Additionally, we have shown that these systems are seen to organize towards synchronization even when no macroscopic signs of global coherence is observed.

Finally, the framework of structured networks has provided a useful benchmark for testing the validity of the parameter r_{link} and the information obtained from the computation of the matrix $\mathcal{D}$. The results obtained by means of these quantities allow us to conclude that for modular networks synchronization is first locally attained at the most internal level of organization and, as the coupling is increased, it

progressively evolves toward the outer shells of the network. The latter process is, however, achieved at the expense of partially readjusting some pairs of synchronized nodes between the inner and outer community levels. Besides, we have obtained evidence that a high cohesion at the first level communities produce a high degree of local synchronization although it delays the appearance of the global coherent state.

This study has extended the previous findings about the paths towards synchronization in complex networks [41] and provides a deeper understanding of phase synchronization phenomena on top of complex topologies. In general, the work supports the idea that in the absence of analytical tools to confront the resolution of nonlinear dynamical models in complex networks, the introduction of new parameters to describe the statistical properties of the emergence of local patterns is needed as they give novel and useful information that might guide our comprehension of these phenomena. On more general grounds, this work adds to other recent findings [54,55] about the topology emerging from dynamical processes. The evidences that are being accumulated point to a dynamical organization, at both the local and global scales, which is driven by the underlying topology. Whether or not this intriguing regularity has something to do with the ubiquity of complex heterogeneous networks in nature is not clear yet. More works in this direction are needed, but we think that they may ultimately lead to uncover important universal relations between the structure and function of complex natural systems that form networks. Another issue to explore in future works concerns the behavior of nonlinear dynamical systems on top of directed networks [56], which will allow deeper insights into the behavior of natural systems.

ACKNOWLEDGMENTS

We thank J.A. Acebrón, S. Boccaletti, A. Díaz-Guilera, C.J. Pérez-Vicente, and V. Latora for helpful comments. J.G.G. and Y.M. are supported by MEC through a FPU grant and the Ramón y Cajal Program, respectively. This work has been partially supported by the Spanish DGICYT Projects Nos. FIS2006-13321-C02-02, FIS2006-12781-C02-01, and FIS2005-00337 and by the European NEST Pathfinder project GABA under Contract No. 043309.

[1] A. Pikovsky, M. Rosenblum, and J. Kurths, *Synchronization: A Universal Concept in Nonlinear Science* (Cambridge University Press, Cambridge, England, 2001).
[2] S. H. Strogatz, Physica D **143**, 1 (2000).
[3] S. C. Manrubia, A. S. Mikhailov, and D. H. Zanette, *Emergence of Dynamical Order. Synchronization Phenomena in Complex Systems* (World Scientific, Singapore, 2004).
[4] L. Glass, Nature (London) **410**, 277 (2001).
[5] A. Pluchino, V. Latora, and A. Rapisarda, Int. J. Mod. Phys. C **16**, 515 (2005).
[6] A. Pluchino, V. Latora, and A. Rapisarda, Eur. Phys. J. B **50**, 169 (2006).
[7] Y. Kuramoto, Lect. Notes Phys. **30**, 420 (1975).
[8] Y. Kuramoto, *Chemical Oscillations, Waves, and Turbulence* (Springer-Verlag, New York, 1984).
[9] A. T. Winfree, J. Theor. Biol. **16**, 15 (1967).
[10] J. A. Acebron, L. L. Bonilla, C. J. Perez Vicente, F. Ritort, and R. Spigler, Rev. Mod. Phys. **77**, 137 (2005).
[11] M. E. J. Newman, SIAM Rev. **45**, 167 (2003).
[12] S. Boccaletti, V. Latora, Y. Moreno, M. Chavez, and D.-U. Hwang, Phys. Rep. **424**, 175 (2006).
[13] H. Jeong, S. P. Mason, A. L. Barabási, and Z. N. Oltvai, Nature (London) **411**, 41 (2001).
[14] R. V. Solé and J. M. Montoya, Proc. R. Soc. London, Ser. B **268**, 2039 (2001).
[15] M. E. J. Newman, Proc. Natl. Acad. Sci. U.S.A. **98**, 404 (2001).
[16] M. Faloutsos, P. Faloutsos, and C. Faloutsos, Comput. Commun. Rev. **29**, 251 (1999).
[17] R. Pastor-Satorras and A. Vespignani, *Evolution and Structure of the Internet: A Statistical Physics Approach* (Cambridge University Press, Cambridge, England, 2004).
[18] F. Wang, Y. Moreno, and Y. Sun, Phys. Rev. E **73**, 036123 (2006).
[19] D. S. Callaway, M. E. J. Newman, S. H. Strogatz, and D. J. Watts, Phys. Rev. Lett. **85**, 5468 (2000).
[20] R. Cohen, K. Erez, D. ben-Avraham, and S. Havlin, Phys. Rev. Lett. **85**, 4626 (2000).
[21] R. Cohen, K. Erez, D. ben-Avraham, and S. Havlin, Phys. Rev. Lett. **86**, 3682 (2001).
[22] R. Pastor-Satorras and A. Vespignani, Phys. Rev. Lett. **86**, 3200 (2001).
[23] R. Pastor-Satorras and A. Vespignani Phys. Rev. E **63**, 066117 (2001).
[24] Y. Moreno, R. Pastor-Satorras, and A. Vespignani, Eur. Phys. J. B **26**, 521 (2002).
[25] D. J. Watts and S. H. Strogatz, Nature (London) **393**, 440 (1998).
[26] L. M. Pecora and T. L. Carroll, Phys. Rev. Lett. **80**, 2109 (1998).
[27] M. Barahona and L. M. Pecora, Phys. Rev. Lett. **89**, 054101 (2002).
[28] T. Nishikawa, A. E. Motter, Y.-C. Lai, and F. C. Hoppensteadt, Phys. Rev. Lett. **91**, 014101 (2003).
[29] H. Hong, B. J. Kim, M. Y. Choi, and H. Park, Phys. Rev. E **69**, 067105 (2004).
[30] M. Chavez, D.-U. Hwang, A. Amann, H. G. E. Hentschel, and S. Boccaletti, Phys. Rev. Lett. **94**, 218701 (2005).
[31] D.-S. Lee, Phys. Rev. E **72**, 026208 (2005).
[32] L. Donetti, P. I. Hurtado, and M. A. Muñoz, Phys. Rev. Lett. **95**, 188701 (2005).
[33] C. Zhou, A. E. Motter, and J. Kurths, Phys. Rev. Lett. **96**, 034101 (2006).
[34] A. E. Motter, C. Zhou, and J. Kurths, Phys. Rev. E **71**, 016116 (2005).
[35] E. Oh, K. Rho, H. Hong, and B. Kahng, Phys. Rev. E **72**,

047101 (2005).
[36] P. N. McGraw and M. Menzinger, Phys. Rev. E **72**, 015101(R) (2005).
[37] A. Arenas, A. Díaz-Guilera, and C. J. Pérez-Vicente, Phys. Rev. Lett. **96**, 114102 (2006).
[38] A. Arenas, A. Díaz-Guilera, and C. J. Pérez-Vicente, Physica D **224**, 27 (2006).
[39] Y. Moreno and A. F. Pacheco, Europhys. Lett. **68**, 603 (2004).
[40] J. Gómez-Gardeñes and Y. Moreno, e-print arXiv:cond-mat/0608309.
[41] J. Gómez-Gardeñes, Y. Moreno, and A. Arenas, Phys. Rev. Lett. **98**, 034101 (2007).
[42] Note that this is only possible in networks with power-law degree distributions, but with a very small probability as $P(k) \sim k^{-\gamma}$ with $\gamma > 0$. In these cases, mean-field solutions independent of N are recovered, with slight differences in the onset of synchronization of all-to-all and scale-free networks [43].
[43] J. G. Restrepo, E. Ott, and B. R. Hunt, Phys. Rev. E **71**, 036151 (2005).
[44] T. Ichinomiya, Phys. Rev. E **70**, 026116 (2004).
[45] J. Gómez-Gardeñes and Y. Moreno, Phys. Rev. E **73**, 056124 (2006).
[46] A direct comparison with the all-to-all Kuramoto model is difficult to establish, since one system is extensive (SF networks) and the other depends on N (KM) so that the results do not correspond to the same effective coupling.
[47] S. N. Dorogovtsev, J. F. F. Mendes, and A. N. Samukhin, Phys. Rev. Lett. **85**, 4633 (2000).
[48] Note that the main difference between both measures is that one refers to the degree of synchronization of nodes (r) with respect to the average phase and the other (r_{link}) to the degree of synchronization between every pair of connected nodes.
[49] Note that the size of the network is relatively small ($N=100$) and thus the critical point is shifted to lower values ($\lambda_c^{ER} \simeq 0.07$ in this case) than that found using a FSS analysis.
[50] L. Danon, A. Diaz-Guilera, J. Duch, and A. Arenas, J. Stat. Mech.: Theory Exp. 2005 P09008.
[51] C. Zhou and J. Kurths, Chaos **16**, 015104 (2006).
[52] M. E. J. Newman, Phys. Rev. E **69**, 066133 (2004).
[53] S. Boccaletti, M. Ivanchenko, V. Latora, A. Pluchino, and A. Rapisarda, Phys. Rev. E **75**, 045102(R) (2007).
[54] J. Gómez-Gardeñes, Y. Moreno, and L. M. Floria, Chaos **16**, 015114 (2006).
[55] J. Gómez-Gardeñes, M. Campillo, L. M. Floria, and Y. Moreno, Phys. Rev. Lett. **98**, 108103 (2007).
[56] M. Timme, Europhys. Lett. **76**, 367 (2006).